The genetic architecture underlying body-size traits plasticity over different temperatures and developmental stages in *Caenorhabditis elegans*

Muhammad I. Maulana[1], Joost A.G. Riksen[1], Basten L. Snoek[1,2], Jan E. Kammenga[1,3], Mark G. Sterken[1,3]

[1]Laboratory of Nematology, Wageningen University, Droevendaalsesteeg 1, 6708 PB Wageningen, The Netherlands

[2]Theoretical Biology and Bioinformatics, Utrecht University, Padualaan 8, 3584 CH Utrecht, The Netherlands

[3]Corresponding authors

Keywords: *Caenorhabditis elegans*, body-size traits, temperature, QTL, plasticity

Abstract

Most ectotherms obey the temperature-size rule, meaning they grow larger in a colder environment. This raises the question of how the interplay between genes and temperature affect the body size of ectotherms. Despite the growing body of literature on the physiological life-history and molecular genetic mechanism underlying the temperature-size rule, the overall genetic architecture orchestrating this complex phenotype is not yet fully understood. One approach to identify genetic regulators of complex phenotypes is Quantitative Trait Locus (QTL) mapping. Here, we explore the genetic architecture of body size phenotypes, in different temperatures using *Caenorhabditis elegans* as a model ectotherm. We used 40 recombinant inbred lines (RILs) derived from N2 and CB4856, which were reared at four different temperatures (16^{o}C, 20^{o}C, 24^{o}C, and 26^{o}C) and measured at two developmental stages (L4 and adult). The animals were measured for body length, width at vulva, body volume, length/width ratio, and seven other body-size traits. The genetically diverse RILs varied in their body-size phenotypes with heritabilities ranging from 0.20 to 0.99. We detected 18 QTL underlying the body-size phenotypes across all treatment combinations, with the majority clustering on Chromosome X. We hypothesize that the Chromosome X QTL could result from a known pleiotropic regulator – *npr-1* – known to affect the body size of *C. elegans* through behavioral changes. In conclusion, our findings shed more light on multiple loci affecting body size plasticity and allow for a more refined analysis of the temperature-size rule.

Introduction

The body temperature of ectotherms such as invertebrates and fish are negatively correlated with their ambient temperature, where warmer environments result in smaller body-size. Besides body-size, the ectotherms' life-history traits are also strongly affected by temperatures. Phenotypic plasticity (the phenotypes that can be expressed by a single genotype at different environmental conditions) due to temperature changes has been studied widely for many different ectotherms, including evolutionary, ecological, physiological, and molecular investigations. In particular, body size plasticity has been studied well, aiming to understand why ectotherms grow larger at lower temperatures, a process called the temperature-size rule (Angilletta & Dunham, 2003; Atkinson 1994). Atkinson 1994 gathered results on the temperature-size rules phenotype in ectotherms from extensive number of studies and showed that 83% of the studies described that colder temperature resulted in significantly bigger body size. Although allelic variants and genes have been found that play an important role in body size plasticity, the genetic architecture underlying this phenomenon is not fully uncovered yet.

Nematodes are not exceptional to this phenomenon. For instance, the nematode *Caenorhabditis elegans*, showed a 33% larger body size when grown at 10^{o}C compared to nematodes grown at 25^{o}C (Van Voorhies, 1996) and other temperatures (i.e 24^{o}C) (Gutteling et al., 2007; Kammenga et al., 2007). Part of this phenotypic variation in lower-temperature-dependent body size was caused by natural genetic variation in the calpain-like protease *tra-3* (Kammenga et al., 2007). Overall, *C. elegans* is an attractive organism for studying the genetics of plasticity to temperature. Its small genome, rapid life cycle (3.5 days at 20^{o}C), genetic tractability, and a wealth of available experimental data have made this nematode a powerful platform to study the genetics underlying complex traits (Gaertner & Phillips, 2010; L. B. Snoek et al., 2020). Besides, *C. elegans* can be maintained completely homozygous,

produce many offspring (200-300 offspring per self-fertilizing hermaphrodite), and can be outcrossed with rarely occurring males (Petersen et al., 2015; Sterken et al., 2015; Gaertner & Phillips, 2010). Furthermore, there are many temperature-related trait differences between two widely used divergent strains: N2 and CB4856. More specifically, studies reported that CB4856 and N2 differed in their response to temperatures in several life-history traits such as time to maturity, fertility, egg size, body size, lifespan, and also in gene expression regulation (Gutteling et al., 2007; Gutteling et al., 2007; Jovic et al., 2017; Kammenga et al., 2007; Li et al., 2006; Rodriguez et al., 2012; Viñuela et al., 2011). Despite these findings, we still do not have a full overview of the loci that affect plasticity at a larger range of different temperatures.

To further elucidate the genetic architecture of temperature affected body size plasticity in *C. elegans*, we selected 40 RILs derived from N2 and CB4856 parents (Li et al., 2006) to study the plasticity and genetic regulation of body-size traits (body-size and some internal organs size) under four temperatures and two developmental stages. First, we sought to investigate the effect of temperature and developmental stages to the genetic parameters (heritability and transgressive segregation) and correlation of the body-size traits. Subsequently, we investigated the genomic regions underlying these body-size traits across temperature-developmental stage combinations. We found 18 QTL of body-size traits. Many of the QTL for different traits colocalized at the same position within temperatures suggesting a pleiotropic effect or close linkage. Moreover, we found colocalizing QTL across temperatures indicating a possible temperature sensitive regulatory mechanism.

Materials and methods

Mapping population

The mapping population used in this study consisted of 40 RILs from a 200 RIL population derived from crossing of N2 and CB4856. These RILs were generated by (Li et al., 2006) and most were genotyped by sequencing, with a genetic map consisting of 729 Single Nucleotide Polymorphism (SNP) markers (Thompson et al., 2015). The strain names and genotypes can be found in Figure S1.

We found that long-range linkage, between markers on different chromosomes, was not present in the population, by studying the pairwise correlation of the genetic markers in the used population (Figure S2).

Cultivation and experimental procedures

C. elegans nematodes were reared following standard culturing practices (Brenner, 1974). RILs were kept at 20^{o}C before experiments and three days before starting an experiment a starved population was transferred to a fresh NGM plate. An experiment was started by bleaching the egg-laying population, following standard protocols (Brenner, 1974). From that point onward, RILs were grown at four different temperatures: 16^{o}C, 20^{o}C, 24^{o}C, or 26^{o}C. At two time-points of developmental stages (L4 and adult) per temperature, microscope pictures (Leica DM IRB, AxioVision) were taken of three nematodes per line per temperature that were mounted on agar pads. The timepoints were chosen such that L4 and young adult nematodes were photographed. The exact times are indicated in the sample data file (Table S1).

Trait measurements and calculations

The number of RILs subjected to treatments per developmental stage was 40, except for treatment of temperature 24°C at L4 stage, where 39 RILs were used. Per life-stage and temperature we took measurements of 3 replicate individuals per RIL, and 6 replicate individuals of the parental lines N2 and CB4856 (from two independent populations). This resulted in 1056 pictures.

To quantify traits, the pictures were loaded into ImageJ (version 1.51f) and traits were manually measured. In total, nine body-size traits were measured: (i) body length, (ii) width at vulva, (iii) length of the pharynx, (iv) width of the pharynx, (v) length of the isthmus, (vi) length of the buccal cavity, (vii) length of the procorpus, (viii) surface postbulb, and (ix) surface nematode. To convert the measurement data from pixels to milimeters (mm), a figure of scale (in mm) was loaded to imageJ. Subsequently, the resolution of *C. elegans* picture and the scale picture were equalized. Next, in ImageJ we determined how many pixels were represented by 0.1 mm. This step was repeated 10 times and the average value was taken as standard conversion scale from pixels to mm. We also calculated body volume (assuming the nematodes body resembles a tube) as

$$V_{body} = \pi * \left(\frac{L_{vulva}}{2}\right) * L_{body}$$

and the length/width ratio (L/W ratio) as the ratio of body length/width at vulva. For none of the traits we have a complete dataset due to difficulties in obtaining accurate measurements, the number of missing values for each trait are as follows: body length = 67; width at vulva = 102; length pharynx = 76; length isthmus = 220; surface postbulb = 219; surface nematode = 232; length buccal cavity =193; length procorpus = 242; body volume = 135; width pharynx = 65; length/width ratio = 135.

For QTL mapping purposes, we defined the phenotypic plasticity of all traits as ratio between the trait mean value at 16°C to 20°C, 20°C to 24°C, and 24°C to 26°C. All raw data can be found in Table S2.

Analytical Software Used

Phenotypic data was analyzed in "R" version 3.5.2x64 using custom written scripts (R core Team 2017). The script is accessible via Gitlab: https://git.wur.nl/published_papers/maulana_2021_4temp. R package used for organizing data was the tidyverse (Wickham et al., 2019), while all plots were made using ggplot2 package (Wickham, 2011), except for heatmaps in Figure S3 which were made using the "heatmap ()" function provided in R. The data was deposited to WormQTL2 where it can be explored interactively (www.bioinformatics.nl/WormQTL2) (Snoek et al., 2020).

Genotype-environment interaction

All phenotypic data were found to be normally distributed, allowing to perform parametric analysis on the data. To determine the effect of RIL lines, temperatures, and developmental stages on the phenotypic traits, full three-way ANOVA was performed, and when appropriate followed by Fisher's LSD *posthoc* test. The traits were regarded as dependent variable with temperatures, developmental stages, and RILs as factors. Significant differences were determined using p-value < 0.05 threshold.

Correlation analysis

The correlation between the traits in all treatment combinations was determined by the Pearson correlation index and plotted in a correlation plot. To correct for the effect of outliers (effect of very high or low value of single observation), we normalized the data as follows:

$$X_{norm,i,j} = \log\left(x_{i,j}/\mu\right)$$

where x is individual observation of the traits in temperature i (16°C, 20°C, 24°C, 26°C)) and developmental stage j (L4, adult) while μ is the mean value of all traits.

Transgressive segregation

To determine transgressive segregation of the traits among RILs panel, we performed multiple t-tests comparing all RIL panel to both parents for all traits per temperature and developmental stages. Transgression was defined when the traits of individual RIL is significantly different than both parents (p.adjust with FDR < 0.05; equal variance not assumed).

Heritability estimation

Broad-sense and narrow-sense heritability of the phenotypic traits over RIL lines was calculated using Restricted Maximum Likelihood (REML) model to explain variation of the traits across the RIL lines (Kang et al., 2008; Rockman et al., 2010). The broad sense heritability was calculated according to the following equation:

$$H^2 = (V_G / (V_G + V_E)$$

where H^2 is the broad-sense heritability, V_G is the genotypic variation explained by the RILs, and V_e is residual variation. The V_G and V_E were estimated by the lme4 model $x_{norm} \sim 1 + (1|strain)$ (Bates et al., 2015).

Narrow-sense heritability is defined as the total variation in the population which is captured by additive effects. We calculated these using the heritability package in R, which estimates narrow-sense heritability based on an kinship matrix (Kruijer et al., 2014). The kinship matrix was calculated using the kinship function from the Emma package in R (Carta et al., 2011; Villanova et al., 2011).

The significances of broad and narrow-sense heritability were determined by permutation analysis where the traits values were randomly assigned to the RILs. Over these permutated values, the variation captured by genotype and residuals were then calculated.

177 This permutation was done 1,000 times for each trait. The result obtained were used as the by-
178 chance-distribution and an FDR= 0.05 threshold was taken as the 50^{th} highest value.
179
180 *QTL mapping*
181 QTL mapping was performed using custom script in R using fitted single marker model as
182 follows:

$$\mu_{i,j} = x_i + E_j$$

183 where μ is the averaged of all strains replicates in terms of their body size-traits *i*, of RIL *j* (N
184 = 40) on marker location x (x= 1, 2, 3, …., 729).
185 Detection of QTL was done by calculating a $-\log_{10}(p)$ score for each marker and each
186 trait. All the values were normalized as $\mu norm_{i,j} = \log(\mu_{i,j})$ where μ is mean value of the
187 traits in temperature *i* (16°C, 20°C, 24°C, 26°C) and developmental stage *j* (L4, adult). To
188 estimate empirical significance of $-\log_{10}(p)$, the traits were randomly permutated value over
189 the RILs 1,000 times. The permutation was done per environment (temperatures)
190 independently, in a similar way as the QTL mapping. The calculation resulted in a
191 significance threshold with false discovery rate (FDR) = 0.05 at a $-\log_{10}(p)$ of 3.4 for QTL
192 detection.

Results

C. elegans body size traits vary across temperatures and developmental stages

To investigate the impact of different genetic background, ambient temperature condition, and developmental stages on the body-size traits, we used a panel of 40 RILs derived from a cross between Bristol strain (N2) and Hawaiian strain (CB4856) (Li et al., 2006). Each individual RIL was grown under four different temperature regimes (16^{o}C, 20^{o}C, 24^{o}C, and 26^{o}C). Once reaching the L4 and adult stage, we took pictures of each RIL with three individual replicates per strain and determined the body size parameters using ImageJ (Figure 1A; see materials and methods).

The eleven body-size traits showed a wide range of variation across RILs, sometimes exceeding their parental strains, suggesting transgressive segregation in the population (Figure 1B; Figure S4). We found that body volume of adult worms in CB4856 did not differ between 16°C and 24°C whereas Bristol N2 grew bigger at lower temperatures. This is in agreement with Kammenga et al., (2007) showing that CB4856 body size was less plastic than N2.

To get insight into the relations between the traits measured, we performed a correlation analysis for all pairs of traits at the two developmental stages. We found that the level of between trait-correlation differed between L4 and adult stage, where temperature seems to be the main driving factor (Figure S3). Both in L4 and adult stage, the body-size traits displayed a strong positive correlation within the same temperature, and strong negative correlation between different temperatures, suggesting that the variation in the body-size traits were temperature specific. Interestingly, both in L4 and adult stage, the body-size traits of worm grown in 16^{o}C and 26^{o}C were separated into several small clusters, while the traits from 20^{o}C and 24^{o}C treatments formed a single positively correlated cluster. These results indicated that there were more similar patterns of variation over RILs in temperature 20^{o}C and 24^{o}C. Strongly correlated body-size traits imply that the same quantitative trait loci could be

detected for these traits due to similar patterns of variation in the RILs, temperatures, and developmental stages. To explore the source of variation of the body-size traits in the RILs population, we used principal component analysis (PCA) (Figure S5). The PCAs describes the variation of the traits based on temperatures and genetic background per developmental stage. At the L4 stage, the first principal component captured 45.5% of the variation that mostly due to 16^{o}C temperature, while the second principal component captured 24% of the variation which derived from 24^{o}C and 26^{o}C temperatures. We found that at L4 stage, the RILs were more similar in lower temperature (16^{o}C) while in 20^{o}C, they were distributed across the PC plot. Subsequently, the value of body-size traits of the nematodes at 24^{o}C were similar to the values at 26^{o}C, but divided into two cluster (Figure S5). On the other hand, the individual RILs did not show any clear clusters at adult stage, indicating there was high variation between the RILs as a result of interaction between environment and genetic background of the RILs. This result combined with the correlation analysis show that there was a substantial variation in the RILs, suggesting that it was possible to detect QTL controlling the traits.

Transgressive segregation and heritability indicate a complex genetic architecture underlying body-size traits

Upon inspecting the distribution of trait variation in the RILs compared to N2 and CB4856, we observed high levels of variation exceeding those of the parental strains (Figure 1B; Figure S4). This suggests transgressive segregation within the RIL population. Hence, we tested the trait values of each RIL versus the parents. We found transgression for almost all traits per temperature-developmental stage combinations (t-test, p.adjust FDR < 0.05) (Table S3). Our findings show that the number of two-sided transgressive RILs depended on the combination of temperature and developmental stage (Figure 2A Figure 2B; Table S3). Whereas in the L4 stage the number of transgressive RILs was constant under 16^{o}C, and

20°C, slightly dropped under 24°C – and then increased at 26°C. Conversely, in the adult stage, the number of transgressive strains decreased as the temperature increased. Moreover, it shows that the parental lines have both positive and negative alleles the interact with the environment leading to a more robust/stable phenotype over a broader temperature range. Using ANOVA, we found that developmental stage was indeed the factor driving transgression ($p = 0.0275$; Table 1) whereas temperature alone showed no relation to the transgression ($p = 0.786$). These findings indicate environment and age-specific effects on the regulation of body-size traits.

Table 1 Results of ANOVA for the number of transgressive lines over temperatures and developmental stages.

Source	Df	Sum Sq	Mean Sq	F value	Pr(>F)
Temperature	3	7.7	2.55	0.35	0.787
Developmental Stage	1	37.0	37.01	5.13	0.028
Temperature*Developmental Stage	3	52.3	17.43	2.41	0.076
Residuals	56	404.4	7.22		

ANOVA: Analysis of variance; Df: degree of freedom

Next, to determine the proportion of variance in body-size traits that were caused by genetic factors, we calculated the broad sense-heritability (H^2) of each trait. We found significant heritability (REML, FDR = 0.05) for 81 out of 88 traits in developmental stage-temperature combinations. The significant heritabilities ranged from 0.20 (width Pharynx at 20°C in L4) to 0.99 (width at 16°C in L4) (Figure 2C; Table S4). Hence, for a large fraction of traits we could detect a high contribution of genetic factors. In addition to broad-sense heritability, we calculated the narrow-sense heritability (h^2) to identify how much of the variation could be explained by additive allelic effects. This analysis suggested that there were 11 traits with significant additive effect (REML, FDR < 0.05; Table S4). For nearly all body-size traits we detected broad-sense heritabilities well beyond narrow-sense heritabilities, indicating a role for epistasis in the genetic architecture of the traits.

Table 2 Results of ANOVA for H^2 of all traits over temperatures and developmental stages

Source	Df	Sum Sq	Mean Sq	F value	Pr(>F)
Temperatures	3	0.292	0.097	2.35	0.078
Developmental Stages	1	0.019	0.019	0.472	0.494
Temperatures*Developmental Stage	3	0.308	0.103	2.487	0.066
Residuals	80	3.308	0.041		

ANOVA: Analysis of variance; Df: degree of freedom

To understand the contribution of temperature and developmental stage on heritability of all traits measured, we conducted an ANOVA (Table 2). The results suggested a trend that the main factor driving heritability was temperature ($p = 0.078$) and its combination with developmental stage ($p = 0.066$). On the other hand, developmental stage showed little relation to the variation of heritability *(*$p = 0.493$). In the adult stage, we observed there were four traits (width at vulva, body length, body volume, and surface area of nematodes) which are relatively robust across all temperatures while in L4 they were found to be more variable across temperature. These four traits ,were affecting each other and observed to be positively correlated (Figure S3). Taken together, overall body-size traits show significant broad-sense heritabilities, indicating a substantial effect of the genetic background on the variation in these traits in this population. Moreover, the correlation between some traits indicate a shared genetic architecture between the traits. These results indicate a higher chance of detecting QTL on the traits measured.

QTL underlying body-size traits in *C. elegans* are influenced by temperature and developmental stages

To identify underlying loci controlling the variation of body-size traits, we performed QTL mapping for all the body-size traits measured in the 40 RILs. Using log-normalized

mean values per RIL as input, we found 18 significant QTL ($-\log_{10}(p) = 3.4$, FDR = 0.05) with $-\log_{10}(p)$ scores ranging up to 6.5 in each temperature and developmental stages (Figure 3, Table S5). We found QTL explaining 28-53% of variance among the RILs (Table S5). We found 7 QTL in the L4 stage namely surface area, length pharynx, body length, length procorpus (detected at 20°C), length/width ratio (detected at 20°C and 24 °C), and surface postbulb (detected at 16 °C) . For the adult stage, 11 QTL were detected for the body-size traits. Here, we found QTL evenly distributed over the temperatures: two at 16°C, two at 20°C, three at 24°C, and four at 26°C (Figure 3A). Of the 18 significant QTL, eight were located on chromosome X, five QTL on chromosome V, three on chromosome I and two on chromosome IV.

We observed QTL-hotspots for various traits. For example, the chromosome I QTL (surface area, body volume, and body length) were positively correlated traits, mapped in the same developmental stage and temperature combination. Hence, this could point to a body-size QTL, where the N2 genotype was associated with larger body size compared to the CB4856 genotype (Figure 3B). Interestingly, all QTL on chromosome V were associated with the size of the feeding-apparatus, were found over various temperatures, and were all associated with an increased size in CB4856 (Figure 3A; Figure S6). In contrast, traits related to the overall body size (e.g. volume) were almost exclusively associated with an increased size due to the N2 allele (Figure 3B).

In line with the indications of the correlation- and heritability analyses, we found evidence for environment (temperatures), age (developmental stage) and genotype interactions. For example, for length/width ratio (Figure. 3C) in the adult stage, significant QTL in chromosome X were detected for the worms grown at 16°C and 24°C, one QTL on chromosome IV for worms grown at 20°C, and no significant QTL detected at 26°C. When we mapped the trait in adult worms grown at 16°C, we found a significant QTL on

chromosome X which we did not find in the L4 stage at 16°C. The same result was found for QTL at temperature 20°C at adult stage on chromosome IV which was not present in L4 stage. Similar patterns of (dis-) appearance were observed for many traits (Figure S7). Hence, traits may be regulated by different set of genes (loci) dependent on temperature-environment and developmental stage. This indicates that there is a considerable effect of genotype-environment interactions.

The RIL population revealed plasticity QTL for several body-size traits

The previous results suggested that QTL affecting body-size traits can be located on different chromosomes when measured in different environment, indicating an environment-QTL interaction. To further understand the mechanism of trait plasticity, we determined trait plasticity using the ratio value of the traits between environments. For QTL mapping, we mapped the plasticity by taking the ratio of measured traits from: 16°C to 20°C, 20°C to 24°C, and 24°C to 26°C as the input data. For all three conditions, we found four significant plasticity QTL. Two plasticity QTL were found in the temperature range from 16°C to 20°C, while one plasticity QTL was found in both temperature range of 20°C to 24°C, and 24°C to 26°C. The two plasticity QTL in in the range between 16°C to 20°C harbouring a locus associated to width pharynx at adult stage, and length of the procorpus at adult stage. Two QTLs were detected for plasticity in isthmus length (20 °C - 24 °C, adult; 24 °C - 26 °C, L4) (Figure 4A, 4B, 4C; Table S6). Plasticity QTL in the temperature range of 16°C to 20°C related to length procorpus at adult stage has a positive effect of N2 genotype at the peak marker location, whereas the width pharynx plasticity QTL at the same temperature range associated to CB4856 genotype. In temperature range 20°C to 24°C, the plasticity QTL related to length isthmus of the nematodes at adult stage was associated to N2 genotype. In contrast, length isthmus of the nematodes at L4 stage in temperature range of 24°C to 26°C was

associated to CB4856 genotype. This indicates that temperature-related phenotypic plasticity of most body-size traits was not governed by alleles with large changes in effect-sizes over the temperature gradient. Rather, it indicates that in general, temperature-related plasticity is due to small increases in loci effects over the course of the gradient.

Discussion

Correlation between body-size traits in *C. elegans* are temperature-specific

In most ectotherms, temperature is an important factor driving body size and is related to life history traits (Angilletta & Dunham, 2003; Ellers & Driessen, 2011). This was also found for *C. elegans* (Gutteling et al., 2007a,b; Kammenga et al., 2007). In this study, we used a *C. elegans* RIL population to study the underlying genetic regions that regulate the body-size traits, both main body traits (i.e length, width at vulva, volume, length/width ratio, and surface area) as well as internal organs and feeding apparatus (i.e length isthmus, length procorpus, length pharynx, width pharynx, and surface postbulb) in different temperatures at two developmental stages. We found that positive correlation between traits was present only within certain temperatures, not between-temperatures. This result suggests a temperature- and developmental stage specific effect on the correlation among traits which can translate into a shared genetic architecture. A similar phenomenon was reported for body mass and egg size in *C. elegans* which correlated positively at 24^{o}C, yet no correlation detected for these traits was reported at 12^{o}C (Gutteling et al., 2007b). Furthermore, these authors also found a negative correlation between egg size and egg number at 12^{o}C but not at 24^{o}C. This is not surprising since developmental stages (age) and temperature are also known to affect the gene expression level in *C. elegans* that translate into a variation in expression-QTL (eQTL) (Li et al., 2006; Snoek et al., 2017; Viñuela et al., 2010).

Previous studies have reported the effect of temperatures on genetic correlation of several life history traits in different species. Norry & Loeschcke (2002) conducted a selection experiment and found a positive correlation effect of lifespan with temperature and sex in *D. melanogaster* at 25^{o}C where the male flies lived longer. However, this effect was reversed at 14^{o}C in which the male flies were shorter lived. In *C. elegans*, an 18% of increase lifespan due to heat-shock was reported for CB4856 but not for N2, whereas the RILs showed a wide

range of lifespan variation due to heat-shock (Rodriguez et al., 2012). Our results are in agreement of other previous studies (reviewed in Sgro & Hoffmann, 2004) that different environmental conditions result in a different correlation power, suggesting that evolutionary trajectories on trade-offs between traits, especially the traits that are controlled by specific loci, depend strongly on the environmental condition.

Genetic parameters indicate a complex genetic regulation of body-size traits

In a population derived from two diverse parents, it is common to detect extreme phenotypes exceeding way beyond the parents (transgression) (Rieseberg et al.,, 1999). Transgression can represent genetic complexity of a trait, for example due to genetic interaction (epistasis) or it could mean that the trait is controlled by multiple loci with opposite effect combinations in the parental strains resulting in a similar phenotype. For example, transgression has been reported for *C. elegans* life-history traits such as egg size, number of eggs, body length (Andersen et al., 2015; Gutteling et al., 2007b; Kammenga et al., 2007), lifespan (Rodriguez et al., 2012), as well as metabolite levels (Gao et al., 2018), and gene expression (Li et al., 2006). We found transgressive segregation for almost all traits in temperature and developmental stage combinations, indicating a complementary actions of multiple loci underlying these traits.

We then calculated the broad-sense heritability (H^2) to investigate the proportion of variance explained by genetic factors in our RIL population. 81 out of 88 body-size traits in temperature-developmental stage combinations were significantly heritable. We found that the heritability of traits was dynamic across different temperatures and developmental stages. Our estimation of broad-sense heritability for adult body length at 20^{o}C (0.51) was similar to an estimation using another N2 x CB4856 RIL panel, reporting 0.57 (Andersen et al., 2014). In addition, the broad-sense heritability of body volume (0.71) and width at vulva (0.76) in

this study are also similar to (B. L. Snoek et al., 2019), which were 0.77 and 0.75, respectively. Heritability is a population trait characteristic and highly depends on the type of population used and environment. Therefore, the fact that we found similar heritability with previous works indicate that the variation if these traits is quite stable between different mapping population. This could also mean that the relative effect of the micro-environment as well as the stochasticity is small. Furthermore, similar patterns of heritability that changed over temperatures (12^{o}C and 24^{o}C) were reported for body mass (volume), growth rate (body length), age at maturity, egg size, and egg numbers (Gutteling et al., 2007a; Gutteling et al., 2007b). The heritability found in our study for body volume and body size were higher, but with the same pattern, where colder temperature resulted in a higher heritability, meaning that the effect of microenvironment or stochasticity is less compared to warmer temperature.

We found heritability was less variable in the adult stage compared to L4. This may be because the worm atL4 grow relatively faster which causing more variation between individuals. Yet, analysis of variance on the heritability showed that temperature was the most influential driver of heritability. At L4 stage, temperature 16^{o}C and 26^{o}C seemed to lead to a higher heritability value, whereas this pattern was not observe at adult stage. Despite the dynamics of heritability across temperature, we found some traits with robust heritability across temperature in adult stage namely width at vulva, body volume, body length, and surface area of the nematode. These traits were also strongly positively correlated in all temperatures. This means, the genetic loci underlying these traits might not be greatly affected by temperature changes which based on the QTL profile in Figure S7 is the case.

QTL mapping revealed genetic-environment interaction underlying body-size traits

By QTL mapping, we found 18 significant QTL for 88 temperature and developmental stage combinations regulating body-size traits. Here, we showed QTL of some the traits were

411 colocalized in the same location in chromosome. For example, body length and surface area
412 of the nematode in L4 stage at 20^{o}C shared the same genomic region on the left arm of
413 chromosome X. Similarly, the QTL for volume, body length and width at vulva in adult stage
414 at 26^{o}C shared the same location at chromosome I. This is expected since these traits have
415 strong positive correlation. All the colocalized traits showed the same QTL effect where N2-
416 derived loci were associated with an increase in size. It is possible that such co-localized QTL
417 were the result of a single pleiotropic modifier affecting various aspects of the *C. elegans*
418 physiology. On the other hand, this might be the result of unresolved separate QTL (Dupuis &
419 Siegmund, 1999; Gutteling et al., 2007b; Sterken et al., 2020).

420 Some of our QTL matched previous work. As body length at 20^{o}C has been
421 investigated across multiple studies, we used it to cross-reference our mapping. The same
422 location (chromosome X: 4.9 Mb) was mapped in two other studies (Andersen et al., 2014;
423 Andersen et al., 2015). Furthermore, many QTL located in left arm of chromosome X were
424 associated with body length, indicating the alleles controlling these traits might the same or
425 linked with alleles of body length. In other study, using a multi-parent RIL, it was found that
426 loci located in the same position (chromosome X around 4.5 to 5Mb) was associated with
427 length/width ratio which is also related to body length (Snoek et al., 2019). For the same trait,
428 (Snoek et al., 2014) found the QTL in different chromosome (i.e chr IV), meaning that our
429 study has the power to reveal previous undetected QTL.

430 These QTL in chromosome X overlapped with the location of the Neuropeptide
431 receptor 1 (*npr-1)* allele, which encodes the mammalian neuropeptide Y receptor homolog.
432 This allele is a known pleiotropic regulator affecting traits such as lifetime fecundity, body
433 size, and resistance to pathogens mediated by altered exposure to bacterial food (Andersen et
434 al., 2014; Nakad et al., 2016; Reddy et al., 2009; Sterken et al., 2015). The *npr-1* allele affect
435 body-size traits by changing feeding behaviour pattern of the worm due to oxygen

concentration that resulted in different food uptake. CB4856 genotype with the ancestral *npr-1* gene aggregated in low oxygen condition (10%) at the edge of bacterial lawn, that made them underfed and starved. In contrast, the N2 genotype with *npr-1* mutation spread out across bacterial lawn with oxygen concentration 21%, thus has more food compared to CB4856 worms (Andersen et al., 2014; Reddy et al., 2009). Moreover, 7 out of 8 QTL that colocalized in chromosome X has an increase size that are associated with N2 genotype, which support our hypothesis that those seven trait are *npr-1* regulated.

Although not significant, we found potential QTL of body volume and width at vulva of adult nematode at 20^{o}C and 24^{o}C on the left arm of chromosome IV (Figure S7) which overlapped with QTL identified previously for body volume by (Gutteling et al., 2007b; Kammenga et al., 2007) at 24^{o}C using a larger population of RILs, also in chromosome X at 20^{o}C using multi-parental RIL (Snoek et al., 2019). These results indicate that these QTL represent robust and predictable genetic associations with temperature and size.

From 18 significant QTL, 9/18 (50%) were transgressive and six of the transgressive traits were found in L4 stage. In addition, 15/18 (83%) of the QTL had moderate to high heritability (> 0.3). These findings indicate a highly complex genetic regulation of many body-size traits that could involve multiple interaction of different genetic variants. This was supported by the higher value of broad-sense heritability compared to narrow-sense heritability which suggests that the driving factors of most heritable traits were additive loci of opposing effects or genetic interactions.

Mapping of plasticity increments indicates small effect-size changes result in shifting loci

By mapping phenotypic plasticity over adjacent temperatures, we only found four plasticity QTL. We found two QTL over 16^{o}C to 20^{o}C that were related to width pharynx and length procorpus, both in adult stage. On the other hand, we detected one QTL over 20^{o}C to

461 24^{o}C that was related to length isthmus in adult stage and one QTL over 24^{o}C to 26^{o}C
462 associated to length isthmus at L4 stage. These result suggests that the QTL associated
463 plasticity was environment specific, meaning that the candidate genes in the QTL region are
464 differentially expressed depending on environmental conditions (Gutteling et al., 2007b). We
465 found plasticity QTL of width pharynx at adult stage (Figure 4A) and length isthmus at L4
466 stage (Figure 4C) that were not detected before in the normal QTL mapping using single
467 temperature regime which might indicate a locus regulating the trait's expression over
468 different environmental condition.

469 Interestingly, plasticity QTL of length isthmus at L4 stage (Figure 4C) from gradient
470 changes of 24^{o}C to 26^{o}C with higher size was associated to CB4856 genotype colocalized
471 with length/width ratio QTL at adult stage under 24^{o}C where higher size was associated to N2
472 genotype. Furthermore, we also found plasticity QTL of length isthmus at adult stage (Figure
473 4B) from gradient changes of 20^{0}C to 24^{0}C colocalized with length pharynx QTL at adult
474 stage under 16^{0}C with opposite genotype effect. These findings may indicate an allelic
475 sensitivity model underlying plasticity mechanism where loci displaying environmentally
476 based allelic sensitivity (Scheiner, 1993). The fact that these plasticity QTL were colocalized
477 with normal QTL may suggest that the QTL contains loci/allele that is activated when the
478 population in a different environment or in an unusual condition (Paaby & Rockman, 2014).

479 Here, we reported the use of 40 RILs derived from divergent strains N2 and CB4856
480 in identifying the genetic parameters of body-size traits. We showed that in different
481 temperatures regimes, heritability of certain traits could change as a result of environmental
482 pressure. We also showed colocalized QTL of different traits in one region in chromosome X,
483 I, V, and IV that indicates a pleiotropic effect or closely linked loci. Furthermore, we found
484 temperature-specific QTL and plasticity QTL which differentially expressed depending on
485 environmental conditions. Follow up study employing the use of near isogenic line or RIAIL

with selection on *npr-1* gene need to be performed to confirm the effect of detected QTL on the body-size traits. Together, our result showed the effect of different temperature and developmental stages to the complexity of body-size traits in *C. elegans*.

Acknowledgements

The authors thank Simone Ariens for measurements on the microscopy images and Miriam Rodriguez for technical assistance. We thank Anne Morbach (Schlaugemacht.net) for making Figure 1A. We thank Harm Nijveen for assistance with WormQTL2. We thank Lisa van Sluijs for the critical review of the draft manuscript. We thank Fred van Eeuwijk for helpful discussions.

Funding

M.G.S. was supported by NWO domain Applied and Engineering Sciences VENI grant (17282)

Availability of data and materials

The strains used in this study can be requested from the authors. The underlying data is included in the paper and interactively accessible via WormQTL2.

Author contributions

MGS, LBS and JEK conceived and designed the experiments. MGS and JAGR conducted the experiments. MIM analyzed the data with input from MGS. MIM and MGS wrote the manuscript, with input from JEK and LBS. All authors commented on the manuscript.

Reference

Andersen, E. C., Bloom, J. S., Gerke, J. P., & Kruglyak, L. (2014). A Variant in the Neuropeptide Receptor npr-1 is a Major Determinant of Caenorhabditis elegans Growth and Physiology. *PLoS Genetics*, *10*(2). https://doi.org/10.1371/journal.pgen.1004156

Andersen, E. C., Shimko, T. C., Crissman, J. R., Ghosh, R., Bloom, J. S., Seidel, H. S., … Kruglyak, L. (2015). A Powerful New Quantitative Genetics Platform, Combining Caenorhabditis elegans High-Throughput Fitness Assays with a Large Collection of Recombinant Strains. *G3*, *5*(5), 911–920. https://doi.org/10.1534/g3.115.017178

Angilletta, M. J., & Dunham, A. E. (2003). The Temperature-Size Rule in Ectotherms : Simple Evolutionary Explanations May Not Be General. *The American Naturalist*, *162*(3).

Atkinson, D. (1994). Temperature and organism size: a biological law for ectotherms?. *Advances in ecological research*, *25*, 1-58

Bates, D., Mächler, M., Bolker, B. M., & Walker, S. C. (2015). Fitting linear mixed-effects models using lme4. *Journal of Statistical Software*, *67*(1). https://doi.org/10.18637/jss.v067.i01

Brenner, S. (1974). Genetics of the Caenorhabditis elegans. *ChemBioChem*, *4*(8), 683–687. https://doi.org/10.1002/cbic.200300625

Carta, D., Villanova, L., Costacurta, S., Patelli, A., Poli, I., Vezzù, S., … Falcaro, P. (2011). Method for optimizing coating properties based on an evolutionary algorithm approach. *Analytical Chemistry*, *83*(16), 6373–6380. https://doi.org/10.1021/ac201337e

Dupuis, J., & Siegmund, D. (1999). Statistical methods for mapping quantitative trait loci from a dense set of markers. *Genetics*, *151*(1), 373–386.

Ellers, J., & Driessen, G. (2011). Genetic correlation between temperature-induced plasticity of life-history traits in a soil arthropod. *Evolutionary Ecology*, *25*, 473–484. https://doi.org/10.1007/s10682-010-9414-1

Gaertner, B. E., & Phillips, P. C. (2010). Caenorhabditis elegans as a platform for molecular quantitative genetics and the systems biology of natural variation. *Genetics Research*, *92*(5–6), 331–348. https://doi.org/10.1017/S0016672310000601

Gao, A. W., Sterken, M. G., de Bos, J. uit, van Creij, J., Kamble, R., Snoek, B. L., … Houtkooper, R. H. (2018). Natural genetic variation in C. Elegans identified genomic loci controlling metabolite levels. *Genome Research*, *28*(9), 1296–1308. https://doi.org/10.1101/gr.232322.117

Gutteling, E. W., Doroszuk, A., Riksen, J. A. G., Prokop, Z., Reszka, J., & Kammenga, J. E. (2007). Environmental influence on the genetic correlations between life-history traits in Caenorhabditis elegans. *Heredity*, *98*, 206–213. https://doi.org/10.1038/sj.hdy.6800929

Gutteling, E. W., Riksen, J. A. G., Bakker, J., & Kammenga, J. E. (2007). Mapping phenotypic plasticity and genotype – environment interactions affecting life-history traits in Caenorhabditis elegans. *Heredity*, *98*, 28–37. https://doi.org/10.1038/sj.hdy.6800894

Jovic, K., Sterken, M. G., Grilli, J., Bevers, R. P. J., Rodriguez, M., Riksen, J. A. G., … Snoek, L. B. (2017). Temporal dynamics of gene expression in heat-stressed Caenorhabditis elegans. *PLoS ONE*, 1–16.

Kammenga, J. E., Doroszuk, A., Riksen, J. A. G., Hazendonk, E., Spiridon, L., Petrescu, A. J., … Bakker, J. (2007). A Caenorhabditis elegans wild type defies the temperature-size rule owing to a single nucleotide polymorphism in tra-3. *PLoS Genetics*, *3*(3), 0358–0366. https://doi.org/10.1371/journal.pgen.0030034

Kang, M. H., Zaitlen, N. A., Wade, C. M., Kirby, A., Heckerman, D., Daly, M. J., & Eskin, E. (2008). Efficient control of population structure in model organism association mapping. *Genetics*, *178*(3), 1709–1723. https://doi.org/10.1534/genetics.107.080101

Kruijer, W., Boer, M. P., Malosetti, M., Flood, P. J., Engel, B., Kooke, R., … Van Eeuwijk,

559 F. A. (2014). Marker-based estimation of heritability in immortal populations. *Genetics*,
560 *199*(2), 379–398. https://doi.org/10.1534/genetics.114.167916
561 Li, Y., Álvarez, O. A., Gutteling, E. W., Tijsterman, M., Fu, J., Riksen, J. A. G., …
562 Kammenga, J. E. (2006). Mapping determinants of gene expression plasticity by
563 genetical genomics in C. elegans. *PLoS Genetics*, *2*(12), 2155–2161.
564 https://doi.org/10.1371/journal.pgen.0020222
565 Nakad, R., Snoek, L. B., Yang, W., Ellendt, S., Schneider, F., Mohr, T. G., … Schulenburg,
566 H. (2016). Contrasting invertebrate immune defense behaviors caused by a single gene,
567 the Caenorhabditis elegans neuropeptide receptor gene npr-1. *BMC Genomics*, *17*(1), 1–
568 20. https://doi.org/10.1186/s12864-016-2603-8
569 Norry, F. M., & Loeschcke, V. R. (2002). Longevity and resistance to cold stress in cold-
570 stress selected lines and their controls in Drosophila melanogaster. *Journal of*
571 *Evolutionary Biology*, *15*, 775–783.
572 Paaby, A. B., & Rockman, M. V. (2014). Cryptic genetic variation□: evolution ’ s hidden
573 substrate. *Nature Reviews Genetics*, *15*(4), 247–258. https://doi.org/10.1038/nrg3688
574 Petersen, C., Dirksen, P., & Schulenburg, H. (2015). Why we need more ecology for genetic
575 models such as C . elegans. *Trends in Genetics*, *31*(3), 120–127.
576 https://doi.org/10.1016/j.tig.2014.12.001
577 Reddy, K. C., Andersen, E. C., Kruglyak, L., & Kim, D. H. (2009). A polymorphism in npr-1
578 is a behavioral determinant of pathogen susceptibility in C. elegans. *Science*, *323*(5912),
579 382–384. https://doi.org/10.1126/science.1166527
580 Rieseberg, L. H., Archer, M. A., & Wayne, R. K. (1999). Transgressive segregation ,
581 adaptation and speciation. *Heredity*, *83*(June).
582 Rockman, M. V, Skrovanek, S. M., & Kruglyak, L. (2010). Selection at Linked Sites Shapes.
583 *Science*, (October), 372–376. https://doi.org/10.1126/science.1194208
584 Rodriguez, M., Snoek, L. B., Riksen, J. A. G., Bevers, R. P., & Kammenga, J. E. (2012).
585 Genetic variation for stress-response hormesis in C . elegans lifespan. *Experimental*
586 *Gerontology*, *47*(8), 581–587. https://doi.org/10.1016/j.exger.2012.05.005
587 Scheiner, S. (1993). Plasticity as a Selectable Trait□: Reply to Via. *American Society of*
588 *Naturalist*, *142*(2), 371–373.
589 Sgro, C., & Hoffmann, A. (2004). Genetic correlations , tradeoffs and environmental
590 variation. *Heredity*, 241–248. https://doi.org/10.1038/sj.hdy.6800532
591 Snoek, B. L., Sterken, M. G., Bevers, R. P. J., Volkers, R. J. M., van’t Hof, A., Brenchley, R.,
592 … Kammenga, J. E. (2017). Contribution of trans regulatory eQTL to cryptic genetic
593 variation in C. elegans. *BMC Genomics*, *18*(1). https://doi.org/10.1186/s12864-017-
594 3899-8
595 Snoek, B. L., Volkers, R. J. M., Nijveen, H., Petersen, C., Dirksen, P., Sterken, M. G., …
596 Kammenga, J. E. (2019). A multi-parent recombinant inbred line population of C .
597 elegans allows identification of novel QTLs for complex life history traits. *BMC Biology*,
598 1–17.
599 Snoek, L. B., Orbidans, H. E., Stastna, J. J., Aartse, A., Rodriguez, M., Riksen, J. A. G., …
600 Harvey, S. C. (2014). Widespread genomic incompatibilities in Caenorhabditis elegans.
601 *G3: Genes, Genomes, Genetics*, *4*(10), 1813–1823.
602 https://doi.org/10.1534/g3.114.013151
603 Snoek, L. B., Sterken, M. G., Hartanto, M., van Zuilichem, A. J., Kammenga, J. E., de Ridder,
604 D., & Nijveen, H. (2020). WormQTL2: an interactive platform for systems genetics in
605 Caenorhabditis elegans. *Database□: The Journal of Biological Databases and Curation*,
606 *2020*, 1–17. https://doi.org/10.1093/database/baz149
607 Sterken, M. G., Bevers, R. P. J., Volkers, R. J. M., Riksen, J. A. G., Kammenga, J. E., &
608 Snoek, B. L. (2020). Dissecting the eQTL Micro-Architecture in Caenorhabditis elegans.

609 *Frontiers in Genetics*, *11*(November), 1–15. https://doi.org/10.3389/fgene.2020.501376
610 Sterken, M. G., Snoek, L. B., Kammenga, J. E., & Andersen, E. C. (2015). The laboratory
611 domestication of Caenorhabditis elegans. *Trends in Genetics*, *31*(5), 224–231.
612 https://doi.org/10.1016/j.tig.2015.02.009
613 Team, R. C. (2017). R: A language and environment for statistical computing
614 Thompson, O. A., Snoek, L. B., Nijveen, H., Sterken, M. G., Volkers, R. J. M., Brenchley, R.,
615 … Waterston, R. H. (2015). Remarkably divergent regions punctuate the genome
616 assembly of the Caenorhabditis elegans hawaiian strain CB4856. *Genetics*, *200*(3), 975–
617 989. https://doi.org/10.1534/genetics.115.175950
618 Van Voorhies, W. A. (1996). Bergmann size clines: A simple explanation for their occurrence
619 in ectotherms. *Evolution*, *50*(3), 1259–1264. https://doi.org/10.1111/j.1558-
620 5646.1996.tb02366.x
621 Viñuela, A., Snoek, L. B., Riksen, J. A. G., & Kammenga, J. E. (2010). Genome-wide gene
622 expression regulation as a function of genotype and age in C. elegans. *Genome Research*,
623 *20*(7), 929–937. https://doi.org/10.1101/gr.102160.109
624 Viñuela, A., Snoek, L. B., Riksen, J. A. G., & Kammenga, J. E. (2011). Gene Expression
625 Modifications by Temperature- Toxicants Interactions in Caenorhabditis elegans. *PLoS*
626 *ONE*, *6*(9). https://doi.org/10.1371/journal.pone.0024676
627 Wickham, H. (2011). Ggplot2. *Wiley Interdisciplinary Reviews: Computational Statistics*,
628 *3*(2), 180–185. https://doi.org/10.1002/wics.147
629 Wickham, H., Averick, M., Bryan, J., Chang, W., McGowan, L., François, R., … Yutani, H.
630 (2019). Welcome to the Tidyverse. *Journal of Open Source Software*, *4*(43), 1686.
631 https://doi.org/10.21105/joss.01686
632
633

Figures Legends

Figure 1. **(A) Flowchart of experimental overview**. A set of 40 RILs were grown at temperature 16^{o}C, 20^{o}C, 24^{o}C, and 26^{o}C. separately, at L4 and adult stage, individual RIL with 3 replicates per RIL were photographed under microscope. Subsequently, the body-size traits of the RILs were determined using ImageJ. **(B) The mean value per genotype of four *C. elegans* body-size traits** across different temperature and developmental stages. The x-axis represents strains used while y-axis represent the mean value of the individual strains in their respective traits. Both parents are depicted in blue (CB4856) and orange (N2), while the RILs are grey. Treatment combination (temperature x developmental stages) are depicted on the facet above the plot box. AD = Adult; 16:AD = Grown in 16^{o}C and measured at adult stage.

Figure 2. **(A) The number of transgressive lines of eleven body-size traits** in *C. elegans* across temperatures and developmental stages. The traits are on the x-axis while y-axis represents the number of transgressive lines based on multiple t-test of traits in each individual lines against both parents (p.adjust FDR < 0.05). Colours represent the temperatures treatment, corresponding to the legend on the right side. **(B) The number of transgressive traits found in the RIL population** per treatments combination (temperature-developmental stage). The temperature is on the x-axis while y-axis represents how many transgression found within those temperatures. Developmental stages are depicted on the above side of the graph. **(C) Broad-sense vs narrow-sense heritability** of body-size traits across temperature and developmental stages. On the x-axis are narrow sense heritability and y-axis are broad-sense heritability. Colours represent traits as depicted on the legend at the bottom of the plot. Shapes represent the significant of broad-sense heritability: dots= not significant; triangle = significant. The dashed line is added as visual reference.

Figure 3. **(A) QTLs found for body-size traits in the 40 RILs.** The x-axis represents the position of the QTL in mega base pairs (Mbp) for each chromosome and y-axis displays the corresponding significant QTL. In total 18 QTL were found with $-\log_{10}(p)$ score ranging from 3.44 to 6.49 ($-\log_{10}(p)$ threshold 3.4, FDR = 0.05). Shapes represent genotype effect: dots: CB4856; triangles: N2. **(B) Allelic effects of QTL** for body length, body volume, and surface area of the nematode in adult stage at 26°C at the pek marker location. RILs that have N2 marker at this locus relatively have bigger body size compared to those that have CB4856 marker. The genetic variation on chromosome I can explain 30 to 37% of the variation in body length, body volume, and surface nematode at that condition. **(C) QTL profile of length/width ratio**. The QTL analysis were performed across four temperatures (16°C, 20°C, 24°C, 26°C) and two developmental stages (L4 and adult). X-axis displays genomic position in the chromosome corresponding to the box above the line while y-axis represents the $-\log_{10}(p)$ score. Box in the right graph show the developmental stages. Blue line represents QTL at 16°C, light blue line at 20°C, orange line at 24°C, and red line at 26°C. Black-dash line represents $-\log_{10}(p)$ threshold (FDR = 0.05).

Figure 4. **(A) QTL plot of length procorpus and width pharynx at adult stage in temperature range of 16°C to 20°C**. X-axis displays genomic position in the chromosome corresponding to the box above the line while y-axis represents the $-\log_{10}(p)$ score. Black-dash line represents significant $-\log_{10}(p)$ threshold 3.0. **(B) QTL plot of width pharynx at adult stage in temperature range of 16°C to 20°C**. X-axis displays genomic position in the chromosome corresponding to the box above the line while y-axis represents the $-\log_{10}(p)$ score. Black-dash line represents significant $-\log_{10}(p)$ threshold 3.0. **(C) QTL plot of length isthmus at adult stage in temperature range of 20°C to 26°C**. X-axis displays genomic position in the chromosome corresponding to the box above the line while y-axis represents

the -$\log_{10}$(p) score. Black-dash line represents significant -$\log_{10}$(p) threshold 3.0. **(D) QTL plot of length isthmus at L4 stage in temperature range of 24^{o}C to 26^{o}C**. X-axis displays genomic position in the chromosome corresponding to the box above the line while y-axis represents the -$\log_{10}$(p) score. Black-dash line represents significant -$\log_{10}$(p) threshold 4.3 (FDR = 0.05). **Box-plots** next to the QTL plots illustrate the **Allelic effects of the QTL** at the peak marker location. X-axis displays the genotype while y-axis displays the traits explained in box-plots.

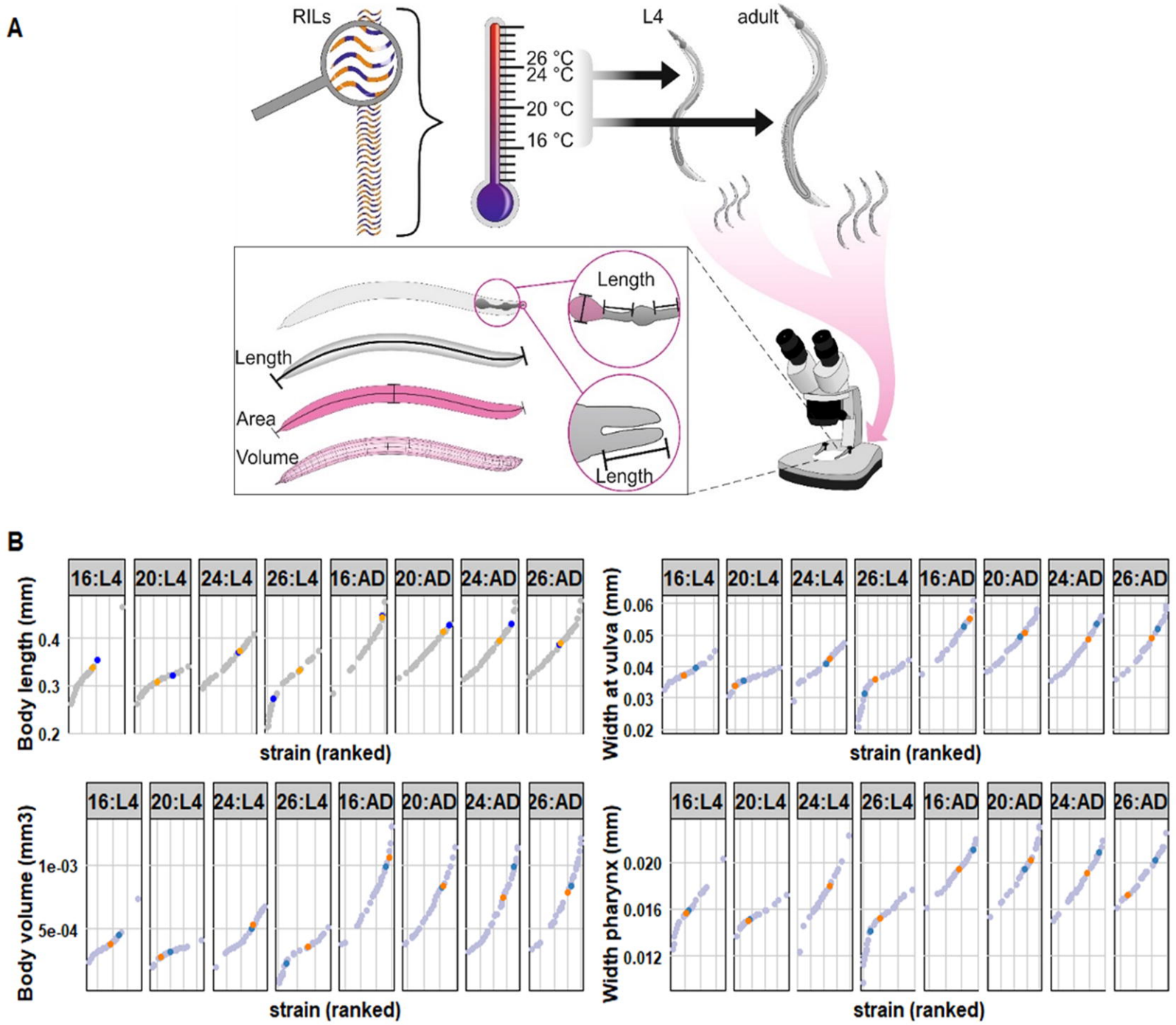
A
RILs
26 °C
24 °C
20 °C
16 °C
L4
adult
Length
Area
Volume
Length
Length
B
16:L4
20:L4
24:L4
26:L4
16:AD
20:AD
24:AD
26:AD
Body length (mm)
0.4
0.3
0.2
strain (ranked)
Width at vulva (mm)
0.06
0.05
0.04
0.03
0.02
strain (ranked)
Body volume (mm3)
1e-03
5e-04
strain (ranked)
Width pharynx (mm)
0.020
0.016
0.012
strain (ranked)

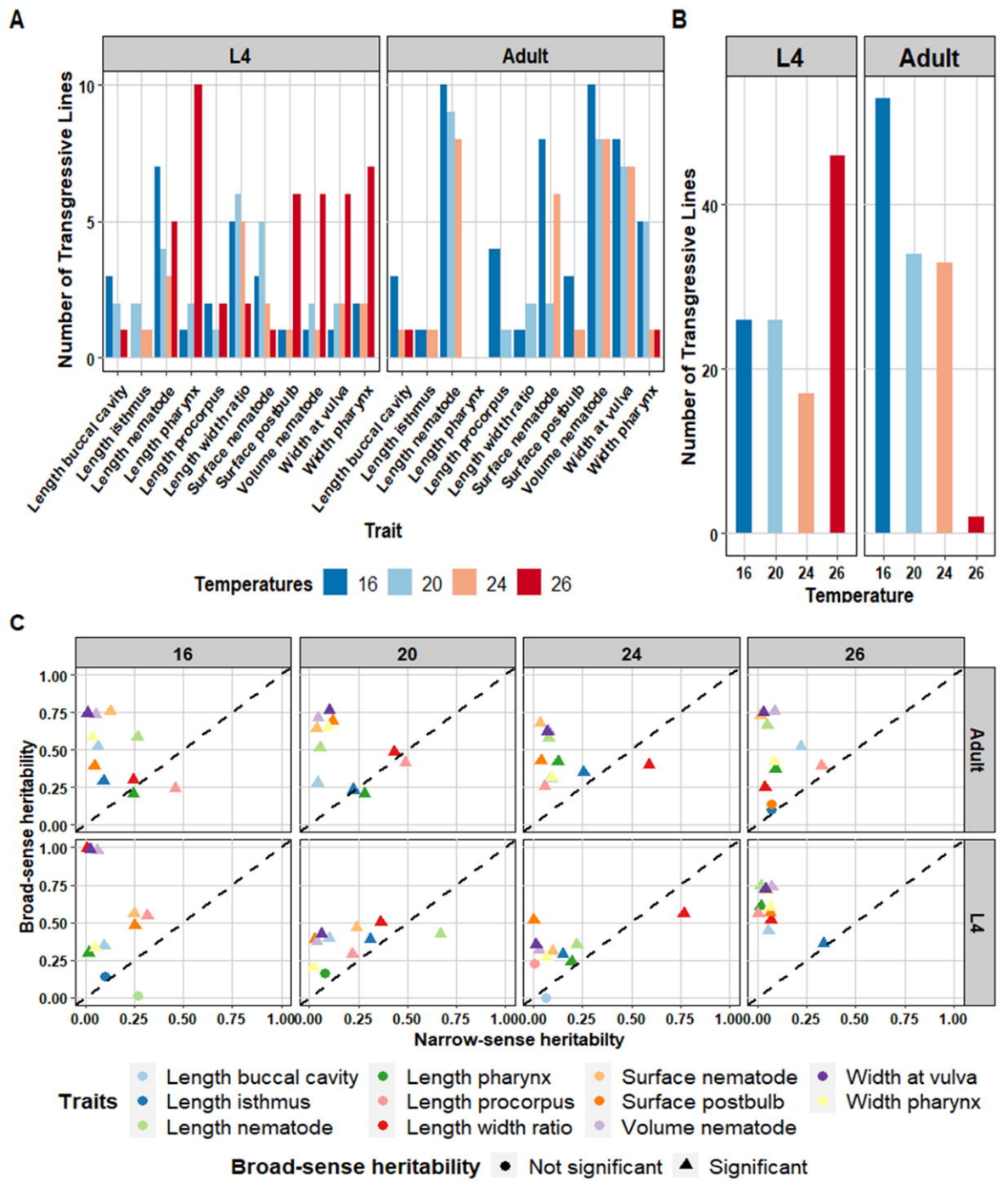
A
L4
Adult
Number of Transgressive Lines
10
5
0
Length buccal cavity
Length isthmus
Length nematode
Length pharynx
Length procorpus
Length width ratio
Surface nematode
Surface postbulb
Volume nematode
Width at vulva
Width pharynx
Trait
Temperatures
16
20
24
26
B
L4
Adult
Number of Transgressive Lines
40
20
0
16
20
24
26
Temperature
C
16
20
24
26
Adult
L4
Broad-sense heritability
1.00
0.75
0.50
0.25
0.00
Narrow-sense heritabilty
Traits
Length buccal cavity
Length isthmus
Length nematode
Length pharynx
Length procorpus
Length width ratio
Surface nematode
Surface postbulb
Volume nematode
Width at vulva
Width pharynx
Broad-sense heritability
Not significant
Significant

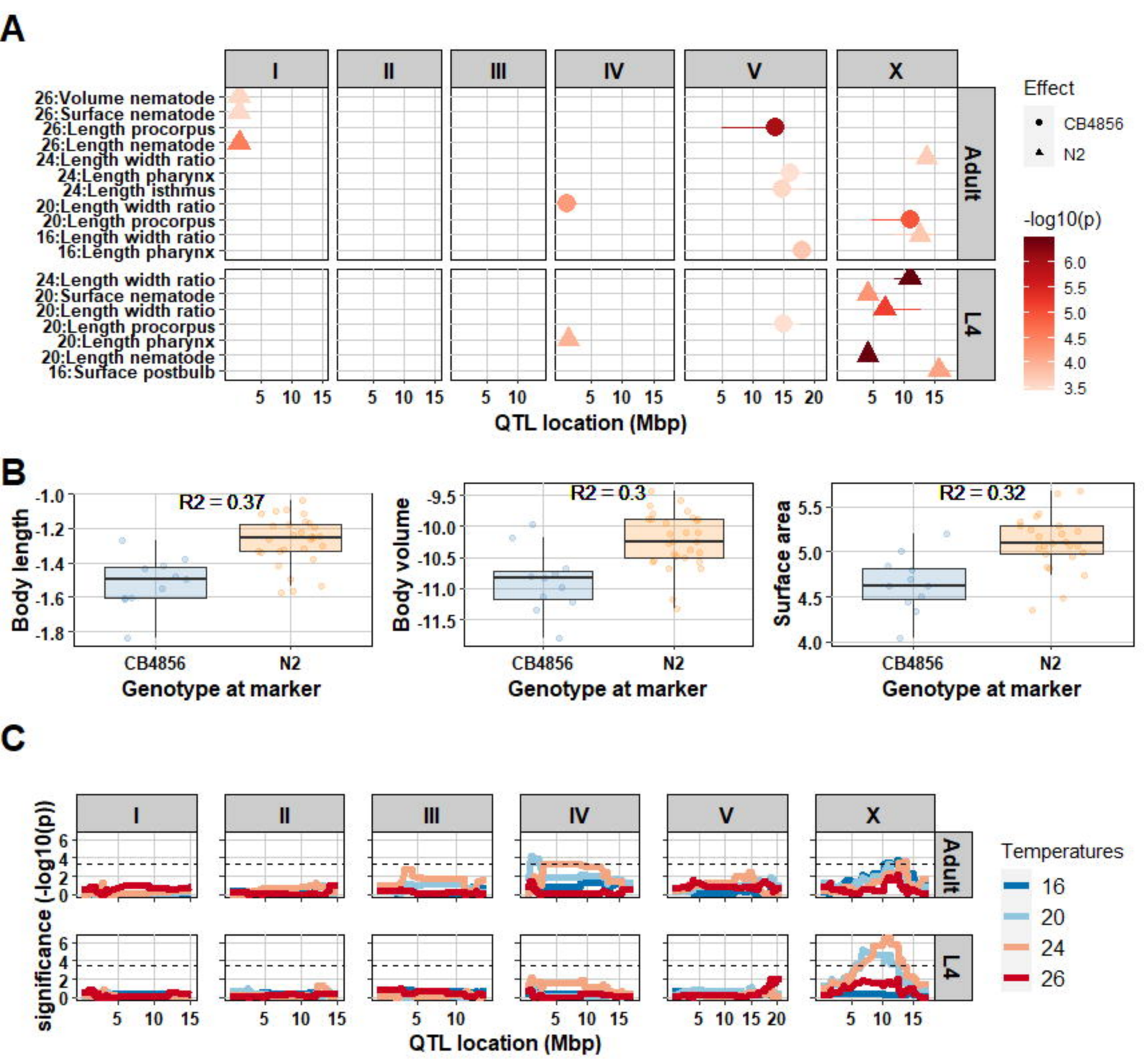
A
I
II
III
IV
V
X
Adult
L4
26:Volume nematode
26:Surface nematode
26:Length procorpus
26:Length nematode
24:Length width ratio
24:Length pharynx
24:Length isthmus
20:Length width ratio
20:Length procorpus
16:Length width ratio
16:Length pharynx
24:Length width ratio
20:Surface nematode
20:Length width ratio
20:Length procorpus
20:Length pharynx
20:Length nematode
16:Surface postbulb
5 10 15
5 10 15
5 10
5 10 15
5 10 15 20
5 10 15
QTL location (Mbp)
Effect
CB4856
N2
-log10(p)
6.0
5.5
5.0
4.5
4.0
3.5
B
Body length
R2 = 0.37
-1.0
-1.2
-1.4
-1.6
-1.8
CB4856
N2
Genotype at marker
Body volume
R2 = 0.3
-9.5
-10.0
-10.5
-11.0
-11.5
CB4856
N2
Genotype at marker
Surface area
R2 = 0.32
5.5
5.0
4.5
4.0
CB4856
N2
Genotype at marker
C
significance (-log10(p))
I
II
III
IV
V
X
Adult
L4
6
4
2
0
5 10 15
5 10 15
5 10
5 10 15
5 10 15 20
5 10 15
QTL location (Mbp)
Temperatures
16
20
24
26

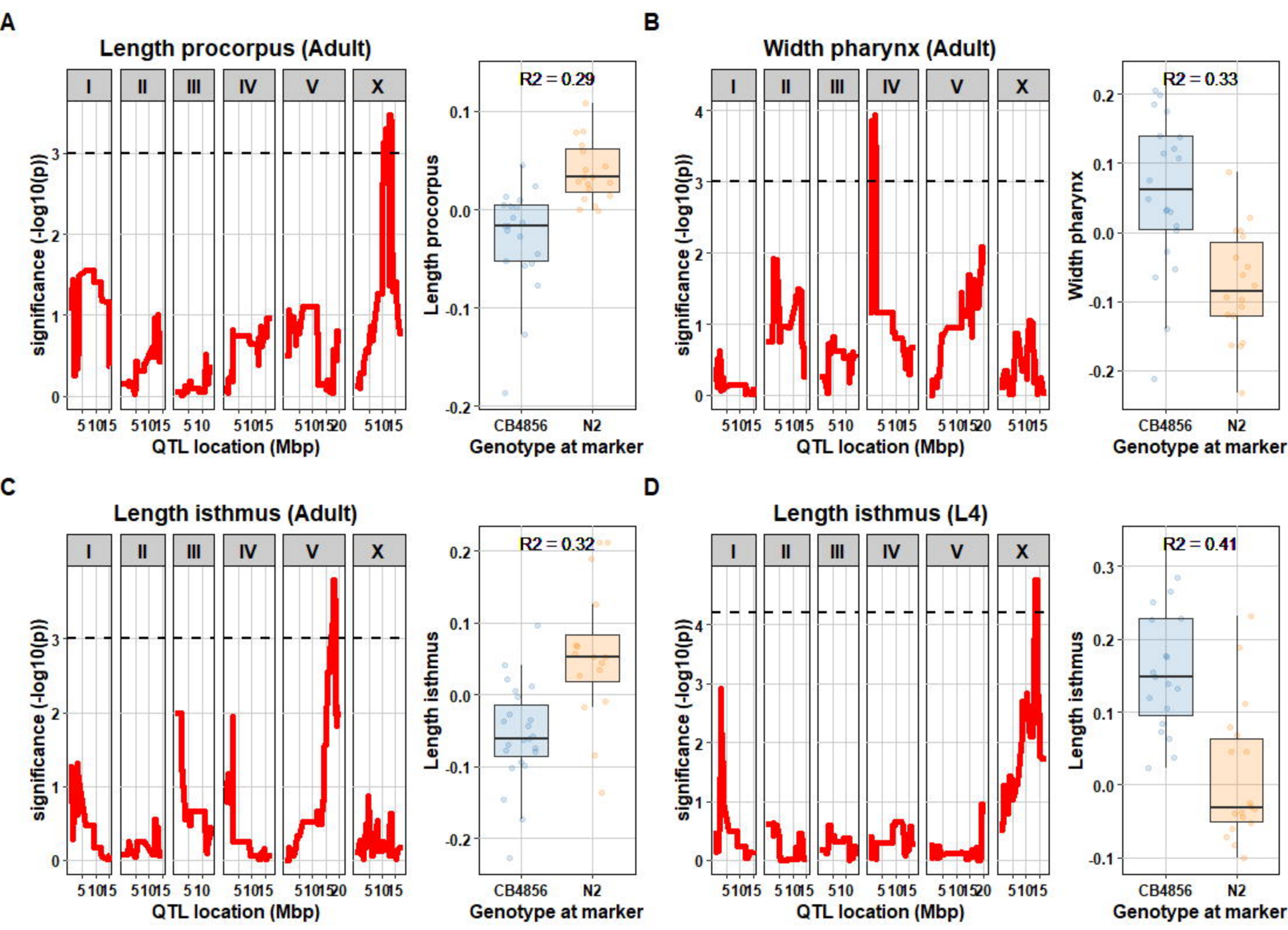
A
Length procorpus (Adult)
I
II
III
IV
V
X
significance (-log10(p))
QTL location (Mbp)
R2 = 0.29
Length procorpus
CB4856
N2
Genotype at marker
B
Width pharynx (Adult)
R2 = 0.33
Width pharynx
C
Length isthmus (Adult)
R2 = 0.32
Length isthmus
D
Length isthmus (L4)
R2 = 0.41